Experimental Validation of Numerically Simulated Unsteady Flow

K.J. Maki [*]   R.F.Beck [*]   A.W. Troesch [*]

29 May - 1 June 2005

Introduction

The numerical simulation of natural unsteady flow always faces the question of whether the solution has satisfied convergence. The common criteria in numerical simulations normally refers to spatial or grid convergence. This is satisfactorily shown by comparing solutions on different grid densities. Once two solutions agree, the grid is accepted as 'dense enough'.

In unsteady flow, the next step is to satisfy temporal convergence. The first step would be to compare solutions on a given grid in a statistical sense. Initially, the mean and variance (RMS), and then higher order moments of the probability distribution of the solution could be used as metrics of convergence. In this paper, we will discuss convergence in space and time using a time-accurate Navier Stokes solver. The convergence of the numerical solver will be compared to experiments using the problem of a backward facing step with a free surface. This choice of physical problem exhibits unique behaviors such as having a wavlength of half the linear wavelength, and periodic vortex shedding synonomous to a circular cylinder.

Experiment

The experiments where conducted in the low turbulence free-surface recirculating water channel at the University of Michigan. This channel has a test section of 2m x 1m x 0.5m (l x w x h). Using a contraction of 4:1, the maximum speed in the test section is 2 m/s.

The model is a step that spans the width of the channel. The step height is defined from the bottom edge of the step to the free surface elevation at zero speed, and is controlled by adjusting the volume of water in the channel.

In analogy with transom stern flow, the non-dimensional parameter describing the free surface behavior is the transom draft Froude number (F_t), which is the Froude number calculated with step height, and inflow speed. The range of interest is the pre-ventilation speeds of $1.0 < F_t < 2.0$. In this abstract all results shown are for $F_t = 1.66$.

The experimental data set is a collection of free surface elevation time series, collected at different downstream locations. Three methods of measuring the free surface are used: a sonic wave probe; a wire-capacitance probe; and a laser induced fluorescense system. The sonic probe has a 'footprint' which effectively averages over an area on the free surface (≈ 3 in. dia.). The wire probe was chosen because it is flexible enough to not have any air entrainment on the downstream side, but with this flexibility, its accuracy suffers, and it has its own dynamics. Finally, the optical method should yield the superior results, but presently is a work in progress. Results from the optical measurements will be presented at the workshop.

Numerical Scheme

The numerical simulations use a two-dimensional solver authored by Alessandro Iafrati [1], where the Navier-Stokes equations are solved for two fluids using a Level Set approach to capture the interface. The procedure solves the conservation of mass and momentum equations in a generalized coordinate system. The governing equations appear as follows,

$$\frac{\partial U_m}{\partial \xi_m} = 0 \tag{1}$$

$$\frac{\partial}{\partial t}\left(J^{-1}u_i\right) + \frac{\partial}{\partial \xi_m}\left(U_m u_i\right) = -\frac{1}{\rho}\frac{\partial}{\partial \xi_m}\left(J^{-1}\frac{\partial \xi_m}{\partial x_i}p\right) +$$
$$J^{-1}q_i + \frac{1}{\rho}\frac{\partial}{\partial \xi_m}\left(\mu G^{mn}\frac{\partial u_i}{\partial \xi_n}\right) \tag{2}$$

Where x_i and u_i are cartesian coordinates and velocities respectively. The transformation to a generalized coordinate ξ_m allows for solutions on more sophisticated grids and gives rise to the area flux, U_m, which is the area flux in the ξ_m direction. The area of the cell, J^{-1}, and metric tensor G^{mn} are also products of the coordinate transformation.

The equations are solved using a fractional step approach. The convective term is advanced with a 3rd order Runge-Kutta method, and the diffusive term is integrated using the stable 2nd order Crank-Nicholson method. The pressure term yields the pressure Poisson equation solved with a multigrid method. The code allows for many possibilities for approximating the spatial derivatives, in these simulations the error is at worst second order.

Results

The non-dimesional units presented in the results use the transom draft T, uniform inflow velocity U, and gravity g, such that;

$$t^* = \frac{tU}{T}, \qquad f^* = \frac{fT}{U}, \qquad x^* = \frac{xg}{2\pi U^2}$$

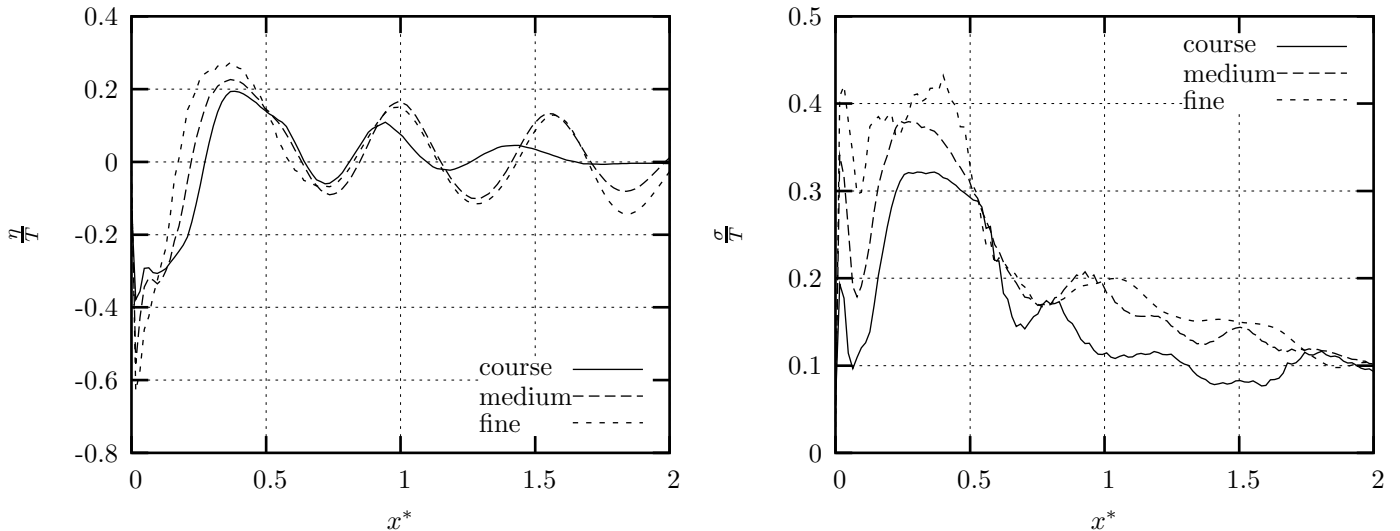[*]The University of Michigan, Ann Arbor, USA

Figure 1: Mean and variance for three different grids, $F_t = 1.66$.

The frequency f^* represents a Strouhal number, and the x^* is the downstream length x divided by the wavelength predicted from the deep water dispersion relation using g and U.

In validation, a suitable metric must be chosen to evaluate the 'quality' of the solution. For this model problem, the mean and variance of the free surface are used. The mean of the free surface $\bar{\eta}$ and variance σ are nondimensionalized with transom draft. To calculate $\bar{\eta}$ and σ for the simulations, the free surface elevation is stored at predetermined time intervals. The length of time record for the course and medium grids is $t^* = 436.8$, and at the time of writing the length of record for the fine grid is $t^* = 109.2$. Then at discrete downstream locations the time average and variance are computed.

To show the quality of spatial convergence, figure (1) shows the mean and variance for the three different grids used in the simulation, namely 64 x 96, 128 x 192, and 256 x 384 cells. The variance increases with the finer meshes, meaning that there is unsteadiness present at smaller scales that the course mesh does not capture.

Figure (1) reveals a very unique feature of this unsteady viscous flow. Linear inviscid wave theory predicts a steady non-dimensional wavelength of $x^* = 1.0$. As seen in figure (1), the steady wavelength is closer to $x^* = 0.5$. The reasons for the shorter wavelength are not obvious. Vanden-Broeck [2] and Scorpio and Beck [3] discuss the attenuation of the linear wavelength due to non-linear effects for transom stern potential flow. Their results show changes that are less than 8%.

To examine the time convergence, discrete time series of the free surface elevation where created. The domain was allowed to fully develop, by waiting until $t^* = 54.6$, which is the time for two 'flow-through' periods between the end of the body, and the begining of the beach. Then the free surface was sampled at a rate of $\Delta t^* = .546$. The mean and variance where computed using four different length of time series, $t^* = 109.2, 218.4, 324.6, 436.8$. Figure (2) demonstrates the time convergence of the simultions.

Finally, the Fourier Transform is used to compare the data in the frequency domain. Figure (3) shows the magnitude of the Fourier coefficients at four downstream locations as compared to experiments, for $F_t = 1.66$. The magnitude is non-dimensionalized with respect to transom draft, and plotted versus non-dimensional frequency f^*. In column A, the numerical results for the medium grid are shown. The figures in column B show the Fourier coefficients for experiments with $T = 7.4\ cm$. The figures in column C are from experiments with $T = 4.5\ cm$. The four downstream locations are $x^* = 0.25, 0.5, 0.75, 1.0$.

Columns A, B, and C all show a peak at $f^* = S_t \approx 0.2$, which is approximately the value for vortex shedding from behind a cylinder. The vortex street that is familiar to the circular cylinder has also been visualized in these experiments, and images will be availible for the workshop. Also, in the two experiments and the simulations the peak decays similarly over the range $x^* < 1.0$.

Columns B, and C while at the same F_t, are at two different R_e (14,000 and 29,000), demonstrating that over this small range the unsteadiness is R_e independent.

References

[1] Iafrati, A., Di Mascio A., Campana, E.F. (2001) *A Level Set Technique Applied to Unsteady Free Surface Flows.* International Journal for Numerical Methods in Fluids, vol. 35.

[2] Vanden-Broeck, J.M. (1980) *Nonlinear Stern Waves.* Journal of Fluid Mechanics, vol. 96, part 3.

[3] Scorpio, S.M., Beck, R.F. (1997) *Two-Dimensional Inviscid Transom Stern Flow.* International Workshop on Water Waves and Floating Bodies.
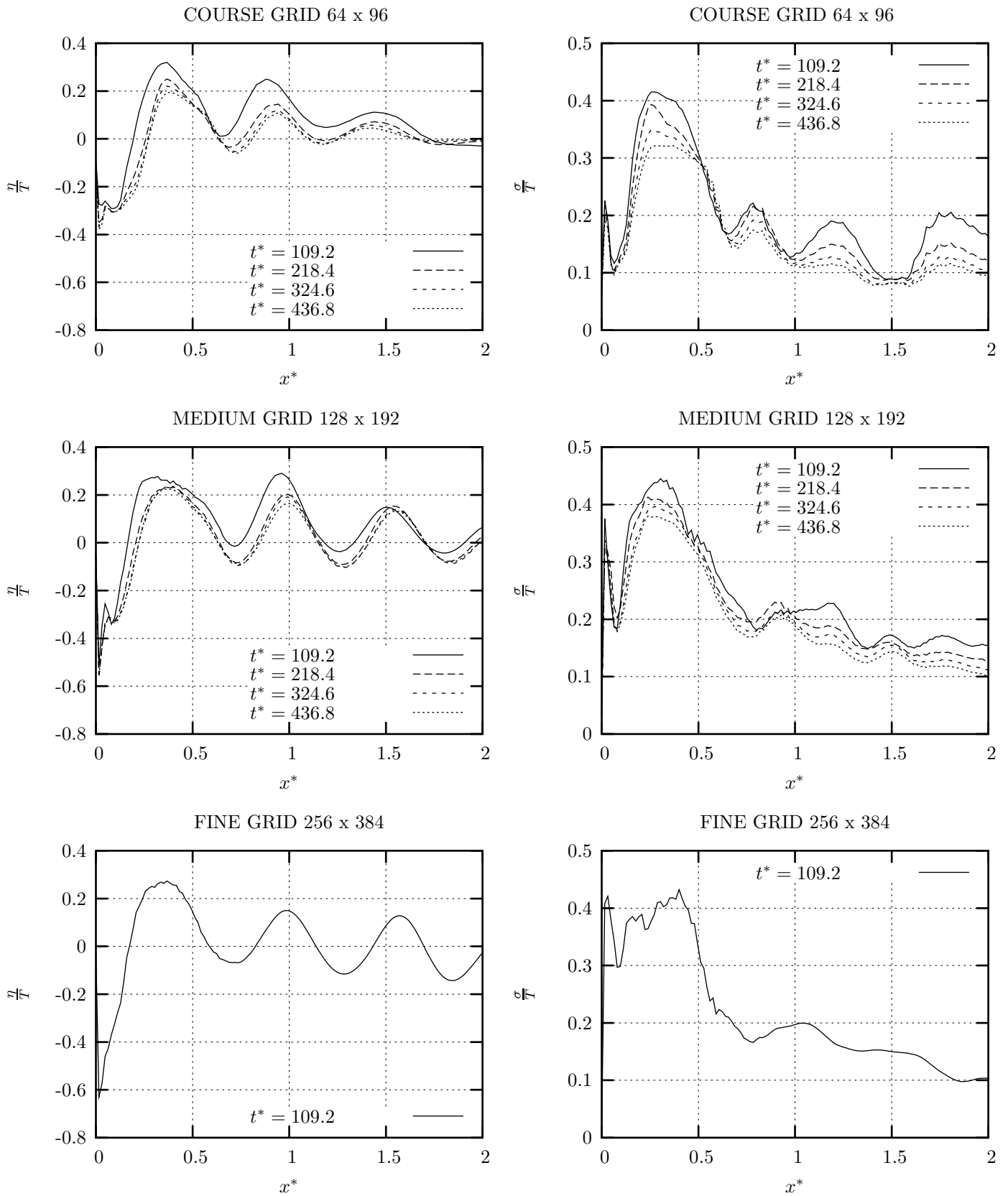
Figure 2: Statistics calculated with four different lengths of time series, $t^* = 109.2, 218.4, 324.6, 436.8$, and for the three different grids. $F_t = 1.66$.
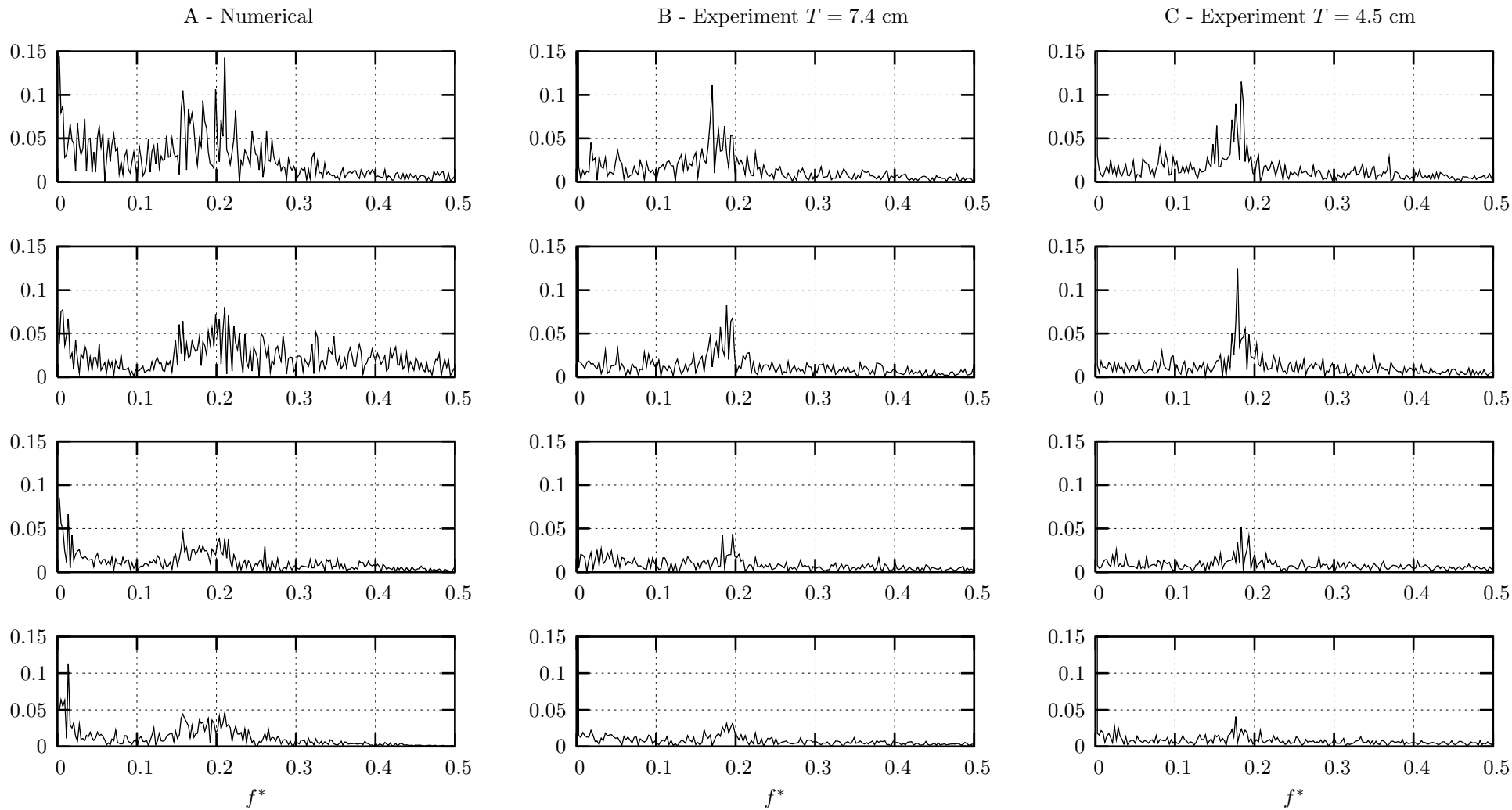
Figure 3: Magnitude of the Fourier coefficient (non-dimensionalized with T) for $F_t = 1.66$ at four different downstream locations, $x^* = 0.25, 0.5, 0.75, 1.0$. Column A: Simulation, medium grid, column B: Experiment using capacitance probe and $T = 7.4\ cm$, column C: Experiment using wire capacitance probe and $T = 4.5\ cm$.